Research Square

Preprints are preliminary reports that have not undergone peer review.
They should not be considered conclusive, used to inform clinical practice,
or referenced by the media as validated information.

TLR3–TICAM1–p38 signalling partially mediates IL-6 induction during human adenovirus type 26 infection in epithelial cells with inhibited clathrin-mediated endocytosis

Isabela Drašković
Ruđer Bošković Institute
Lea Vrbančić
Ruđer Bošković Institute
Davor Nestić
Ruđer Bošković Institute
Ksenija Božinović
Ruđer Bošković Institute
Gabriela N. Condezo
Centro Nacional de Biotecnología
Carmen San Martín
Centro Nacional de Biotecnología
Jerome Custers
Janssen Vaccines and Preventions BV
Dragomira Majhen
dmajhen@irb.hr
Ruđer Bošković Institute

Article

Keywords: Endocytosis, innate immune response, vaccine vectors, TLR, adenovirus

Posted Date: November 11th, 2026

DOI: https://doi.org/10.21203/rs.3.rs-11278287/v1

License: This work is licensed under a Creative Commons Attribution 4.0 International License.
Read Full License

Additional Declarations: No competing interests reported.

TLR3–TICAM1–p38 signalling partially mediates IL-6 induction during human adenovirus type 26 infection in epithelial cells with inhibited clathrin-mediated endocytosis

Drašković Isabela[1], Vrbančić Lea[1*], Nestić Davor[1#], Božinović Ksenija[1], Gabriela N. Condezo[2], Carmen San Martín[2], Custers Jerome[3$], Majhen Dragomira[1,$]

[1]Laboratory for Cell Biology and Signalling, Division of Molecular Biology, Ruđer Bošković Institute, Zagreb, Croatia, [2]Department of Macromolecular Structures, Centro Nacional de Biotecnología (CNB-CSIC), Madrid, Spain, [3]Janssen Vaccines and Preventions BV, Leiden, The Netherlands, *present address: Laboratory for protein dynamics, Division of Molecular Medicine, Ruđer Bošković Institute, Zagreb, Croatia, #current address: Department of Biochemistry, University of Zürich, Zürich, Switzerland, $current address: Vector Bioconsult, Alphen aan den Rijn, The Netherlands

[$]corresponding author

corresponding author e mail: dmajhen@irb.hr

Short title

TLR3 pathway in non-CME HAdV26 infection

Abstract.

Human adenovirus type 26 (HAdV-D26) is a clinically important vector, but the connection between its entry pathway, intracellular trafficking, and innate immune sensing remains unclear. As innate immune sensors are distributed throughout the cell, the virus entry route and subcellular localization likely shape immune activation. Here, we investigated how altered entry routes and endosomal retention of HAdV-D26 influence Toll-like receptor (TLR)-mediated signalling in epithelial cells. Using A549 cells with inhibited clathrin-mediated endocytosis (CME) or *de novo* αvβ3 integrin expression, we analysed IL-6 and IL-8 expression following HAdV-D26 infection and examined the underlying signalling mechanisms. In CME-inhibited A549 cells, where HAdV-D26 persisted longer in early endosomes, HAdV-D26 infection induced IL-6 expression partially through a TLR3–TICAM1–p38-dependent mechanism. Inhibition of TLR3 or p38, as well as knockdown of TICAM1, reduced the elevated IL-6 response observed under CME inhibition. In contrast, inhibition of TLR4 or knockdown of MyD88 increased HAdV-D26-induced IL-6 and IL-8 expression in A549 cells, indicating a negative regulatory role of TLR4–MyD88 signalling. Furthermore, MyD88 knockdown reduced IL-8 expression in A549 cells with *de novo* αvβ3 integrin expression, linking integrin-mediated entry to MyD88-dependent signalling. In conclusion, these findings highlight how entry pathway and intracellular localization shape innate immune sensing of adenoviral vectors.

Key words

Endocytosis, innate immune response, vaccine vectors, TLR, adenovirus

Introduction.

Human adenoviruses (HAdVs) are non-enveloped double-stranded DNA viruses that are widely used as vectors for vaccination and gene delivery [1]. Adenovirus infection is initiated

by binding to cellular receptors, followed by internalization and intracellular trafficking toward the nucleus. Alterations in entry routes and trafficking pathways can influence the efficiency of endosomal escape, cytoplasmic localization, overall infectivity [2] and innate sensing [3].

Innate immune responses to viral infection depend on how viruses enter cells and where viral components localize intracellularly. Innate immune recognition of viral infection is mediated by pattern recognition receptors (PRRs) that are spatially segregated within the cell [4]. The best described PRRs are Toll-like receptors (TLRs) located both on the cell surface and within endosomes [5]. Endosomal TLRs detect viral nucleic acids within vesicular compartments, whereas cytosolic PRRs recognize viral components following endosomal disruption or escape [6]. Engagement of distinct PRRs can result in qualitatively different signalling outcomes [7] therefore, the route of viral entry and the intracellular localization of viral components are critical determinants of innate immune activation.

HAdV-D26 is clinically relevant as a vaccine vector [8], yet how its entry, trafficking, and endosomal localization influence innate immune activation remains unclear. We previously showed that inhibition of clathrin-mediated endocytosis (CME) increases HAdV-D26 binding, internalization, and transduction without altering its receptor, integrin αvβ3 [9] and that elevated αvβ3 expression similarly enhances infection [10]. However, whether HAdV-D26 engages TLR-mediated innate immune signalling, particularly via endosomal TLRs, remains unknown.

Therefore, the present study addresses this gap by investigating how increased intracellular availability and different subcellular localization of HAdV-D26 influence innate immune activation and TLR-associated signalling in epithelial cells**.** We analysed IL-6 and IL-8 expression, cytokines known to be upregulated upon HAdV-D26 infection [11], in either CME-inhibited A549 cells or A549 cells with *de novo* αvβ3 integrin expression infected with HAdV-D26 and investigated the underlying molecular mechanism.

We found that in CME-inhibited A549 cells, in which HAdV-D26 stays longer in early endosomes than in control A549 cells, infection induces IL-6 expression in TLR3-, TICAM1- and p38-mediated fashion. Namely, inhibition of TLR3, knockdown of TICAM1, or inhibition of p38 reduced otherwise increased HAdV-D26-induced IL-6 expression in CME-inhibited A549 cells. TLR3 signalling was also involved in IL-8 expression in both, A549 cells and CME-inhibited A549 cells infected with HAdV-D26. Interestingly, TLR4 inhibition and MyD88 knockdown further increased HAdV-D26-induced IL-6 and IL-8 expression in A549 cells, suggesting that TLR4–MyD88 signalling exerts a negative regulatory effect on pro-inflammatory cytokine production in this context. In A549 cells with *de novo* αvβ3 integrin expression, MyD88 knockdown decreased HAdV-D26-induced IL-8 expression, implying that integrin-mediated HAdV-D26 cell entry triggers signalling other than TLR3 or TLR4-mediated.

By linking viral entry and trafficking to immune sensing, this study provides mechanistic insight into how host cells detect HAdV-D26 and how altered entry routes shape innate responses. These insights inform adenovirus biology and support the rational optimization of adenoviral vectors [12, 13] as modulating entry or trafficking may help fine-tune immunogenicity, improve vaccine efficacy, and limit excessive inflammation. Thus, our findings have implications for both antiviral immunity and the development of safer and more effective adenoviral therapeutics.

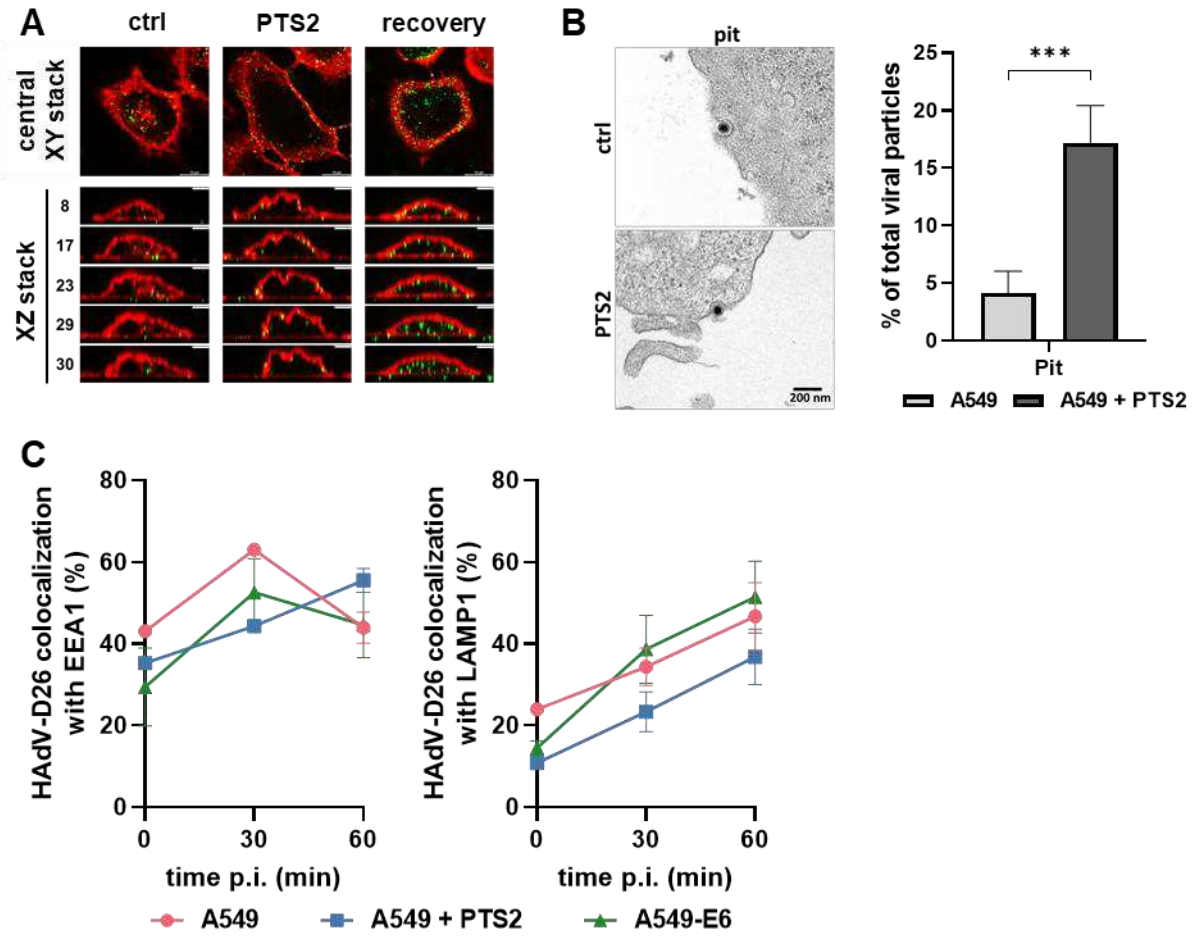
Results.

Inhibition of clathrin-mediated endocytosis alters endosomal trafficking of HAdV-D26, while αvβ3 integrin promotes early endosomal escape. In our previous work, we observed that inhibition of clathrin-mediated endocytosis (CME-inhibited cells; cells treated with Pitstop2 (PTS2; [14]) [9] or *de novo* overexpression of αvβ3 integrin in A549 cells [10], increased HAdV-D26 binding, cellular uptake and transduction efficiency (Table 1). CME-inhibited A549 cells allow investigation of HAdV-D26–host interactions under conditions of impaired clathrin-mediated endocytosis, resulting in viral retention at the plasma membrane without increased αvβ3 integrin expression. *De novo* increased expression of αvβ3 integrin promotes integrin-mediated HAdV-D26 uptake. Together, these models enable the separation of receptor engagement, internalization route, and downstream innate immune signalling.

Table 1. Description of cell models used in this study.

Cell model	Key alteration	Observed effect	Ref.
A549	Baseline CME Baseline expression αvβ3	Baseline HAdV-D26 binding Baseline HAdV-D26 transduction efficiency	10
A549+PTS2	Inhibited CME Baseline expression αvβ3	Increased HAdV-D26 binding Increased HAdV-D26 transduction efficiency HAdV-D26 retained in the proximity of cell membrane	9
A549-E6	Baseline CME *De novo* increased expression αvβ3	Increased HAdV-D26 binding Increased HAdV-D26 transduction efficiency	9

Because entry pathway and receptor usage influence endosomal routing, we examined the temporal localization of HAdV-D26 in early and late endosomes under CME inhibition or αvβ3 integrin overexpression. Inhibition of CME stalled HAdV-D26 in the proximity of the cell membrane (Figure 1A) and increased the amount of HAdV-D26 in pits (Figure 1B). In the A549-E6 cells, HAdV-D26 shows only a modest reduction in localization to EEA1-positive endosomes and a slight increase in LAMP1-positive compartments compared with A549 cells, while following a similar temporal trend (Figure 1C and S1). In contrast, in CME-inhibited A549 cells, viral particles remain associated with EEA1-positive endosomes for longer and do not show the decline observed after 30 min, which may explain their reduced accumulation in late endosomes/lysosomes.



111

112

113 **Figure 1. Inhibition of CME or *de novo* expression of αvβ3 integrin alters the time-**
114 **dependent localization of HAdV-D26 in early and late endosomes/lysosomes in A549 cells.**
115 (A) Confocal images of HAdV-D26 retained near the cell membrane in CME-inhibited A549
116 cells, 60 min p.i. A representative XY optical section through the cell center is shown, with
117 corresponding XZ orthogonal views at the indicated positions. Green, virus; red, cell membrane
118 (WGA); yellow, colocalization of virus and membrane. Scale bar=10 µm. (B) Representative
119 TEM images and corresponding quantification of HAdV-D26 localization in pits in CME-
120 inhibited A549 cells. Data are presented as the mean ± SEM. (C) Quantification of
121 colocalization of HAdV-D26 with early endosome (EEA1) and late endosome/lysosome
122 (LAMP1) at the indicated time points in A549, CME-inhibited A549 (A549 + PTS2) or A549
123 cells with *de novo* expression of αvβ3 integrin (A549-E6). Data are presented as the mean ±
124 SD.

125

126 **Altered HAdV-D26 trafficking differentially modulates early expression of IL-6 and IL-**
127 **8 in A549 cells.** To investigate how HAdV-D26 localization in different endosomal
128 compartments affects early innate immune responses IL-6 and IL-8 mRNA levels were
129 quantified 60 minutes post infection (p.i.). In A549 and CME-inhibited A549 cells, HAdV-
130 D26 infection induced a 2.3-fold and 2.9-fold increase in IL-6 mRNA levels, respectively,
131 compared with their corresponding non-infected controls. In contrast, in A549 cells with *de*

novo αvβ3 integrin expression, HAdV-D26 infection did not alter IL-6 mRNA levels (Fig. 2A). IL-8 mRNA levels were increased in A549 cells infected with HAdV-D26, while in CME-inhibited cells or cells with *de novo* expression of αvβ3 integrin we did not observed any change in IL-8 expression following HAdV-D26 infection (Fig. 2B). Notably, both CME inhibition and *de novo* αvβ3 integrin expression increased basal IL-6 and IL-8 mRNA levels.

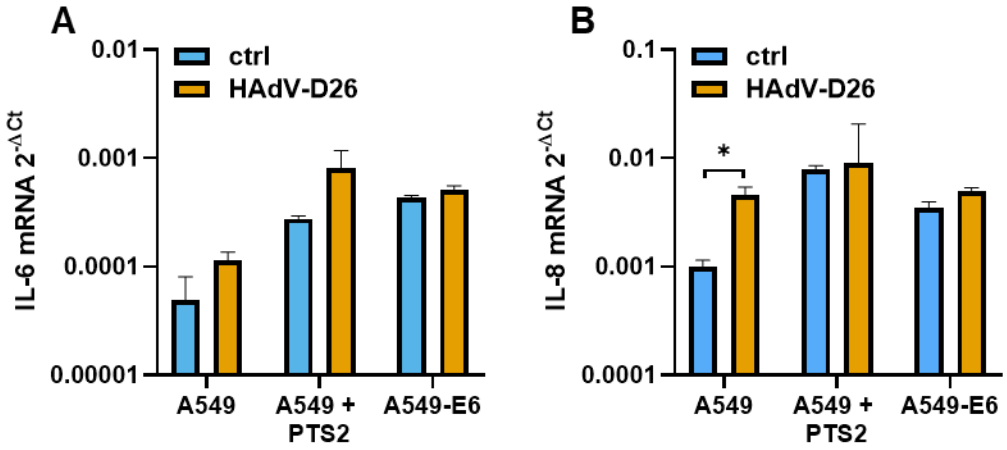


Figure 2. CME inhibition and *de novo* αvβ3 integrin expression differently modulate IL-6 and IL-8 mRNA in HAdV-D26-infected A549 cells. (A) IL-6 and (B) IL-8 mRNA levels measured by qPCR in A549, CME-inhibited A549 (A549 + PTS2) or A549 cells with *de novo* expression of αvβ3 integrin (A549-E6) at 60 min p.i. with HAdV-D26 (MOI 10^4 vp/cell). Data are presented as the mean ± SD.

Context-dependent MyD88- and TICAM1-mediated regulation of HAdV-D26-induced IL-6 and IL-8. The innate immune system detects viruses via PRRs that recognize pathogen-specific patterns, triggering signaling pathways that induce cytokine expression. Given the established role of TLR9 in adenovirus sensing [15, 16], we sought to define the downstream TLR signaling pathways involved in cytokine induction following HAdV-D26 infection by focusing on the adaptor proteins MyD88 and TICAM1 [17].

In A549 cells with *de novo* expression of αvβ3 integrin, MyD88 knockdown (Fig. S2A) reduced HAdV-D26–induced IL-8 expression by 1.7-fold, but had no effect on IL-6 or IL-8 expression in CME-inhibited A549 cells (Fig. 3A and 3B). Unexpectedly, in A549 cells, MyD88 knockdown increased HAdV-D26-induced IL-6 (4.2-fold) and IL-8 (2.5-fold) expression (Fig. 3A and 3B). TICAM1 knockdown (Fig S2B) reduced both HAdV-D26 induced IL-6 (1.9-fold) and IL-8 (1.5-fold) expression in CME-inhibited A549 cells (Fig. 3C and 3D), and IL-8 (2.1-fold) in A549 cells. TICAM1 knockdown had no effect on HAdV-D26-induced IL-6 or IL-8 expression in A549 cells with *de novo* αvβ3 integrin expression.

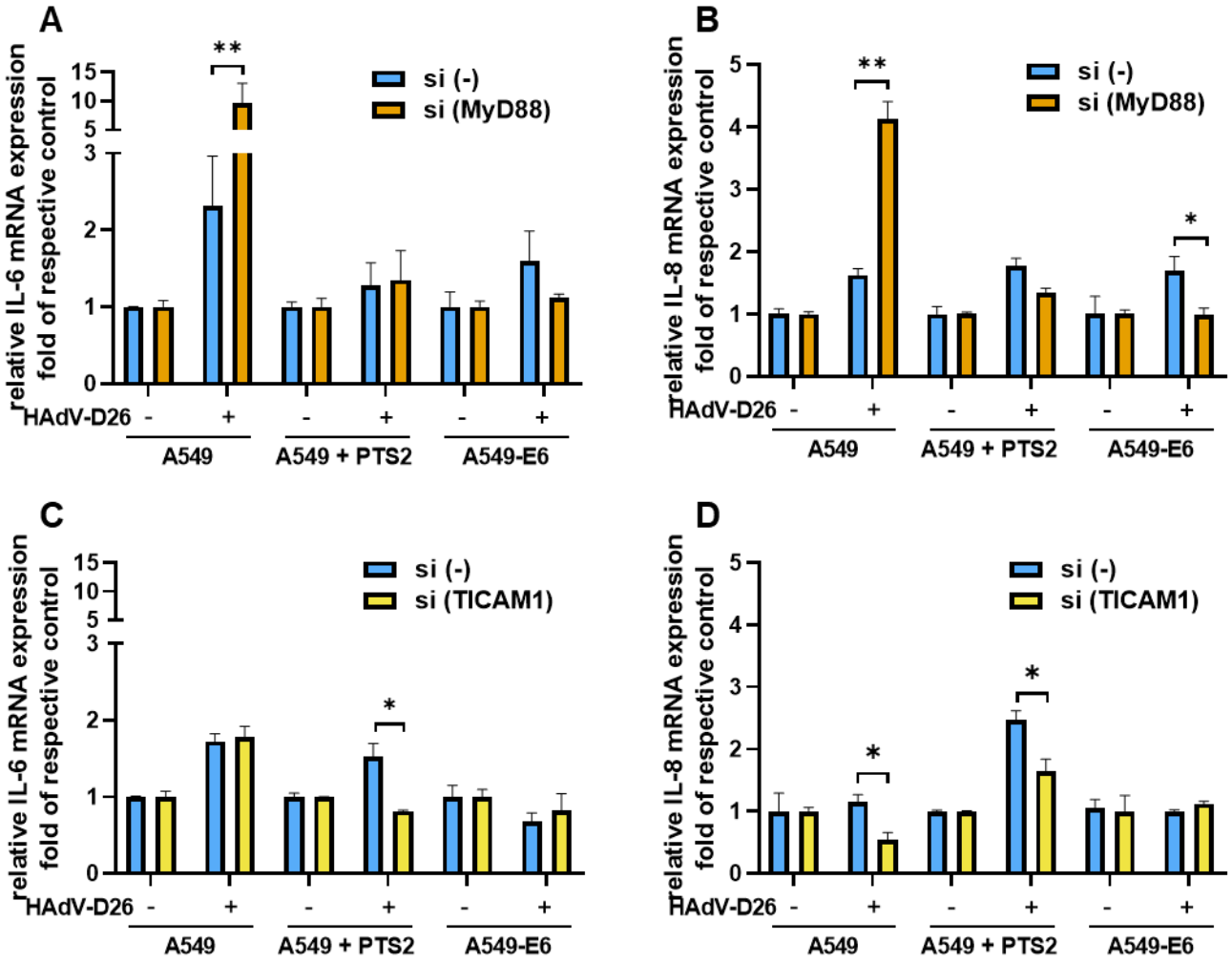


Figure 3. **Role of MyD88 and TICAM1 in regulating HAdV-D26–induced IL-6 and IL-8 expression depends on receptor usage, route of viral entry and intracellular trafficking.** IL-6 and IL-8 mRNA levels measured by qPCR in MyD88 (A and B) or TICAM1 (C and D) depleted A549, CME-inhibited A549 (A549 + PTS2) or A549 cells with *de novo* expression of αvβ3 integrin (A549-E6) at 60 min p.i. with HAdV-D26 (MOI 10^4 vp/cell). Data are presented as the mean ± SD, normalized to si(-) with no virus.

TRL3 is partially involved in HAdV-D26-induced expression of IL-6 and IL-8. All TLRs engage MyD88, except TLR3, which signals exclusively via TICAM1, while TLR4 engages MyD88 or TICAM1 depending on weather it is located at the cell surface or in endosomes. Since we saw the implication of both MyD88 and TICAM1 in HAdV-D26-induced IL-6 and IL-8 expression, we wanted to further analyse the role of TLR3 and TLR4 in HAdV-D26 sensing by using selective TLR3 (CU-CPT 4a) or TLR4 (TAK-242) inhibitors. Inhibiting TLR3 (Fig. S2C) decreased HAdV-D26-induced IL-6 (1.5-fold) expression in CME-inhibited A549 cells and IL-8 (1.9-fold) expression in A549 cells (Fig. 4A and 4B). On the other hand, TLR4 inhibition (Fig. S2D) resulted in increased IL-6 (1.6-fold) and IL-8 (1.9-fold) expression in A549 cells.

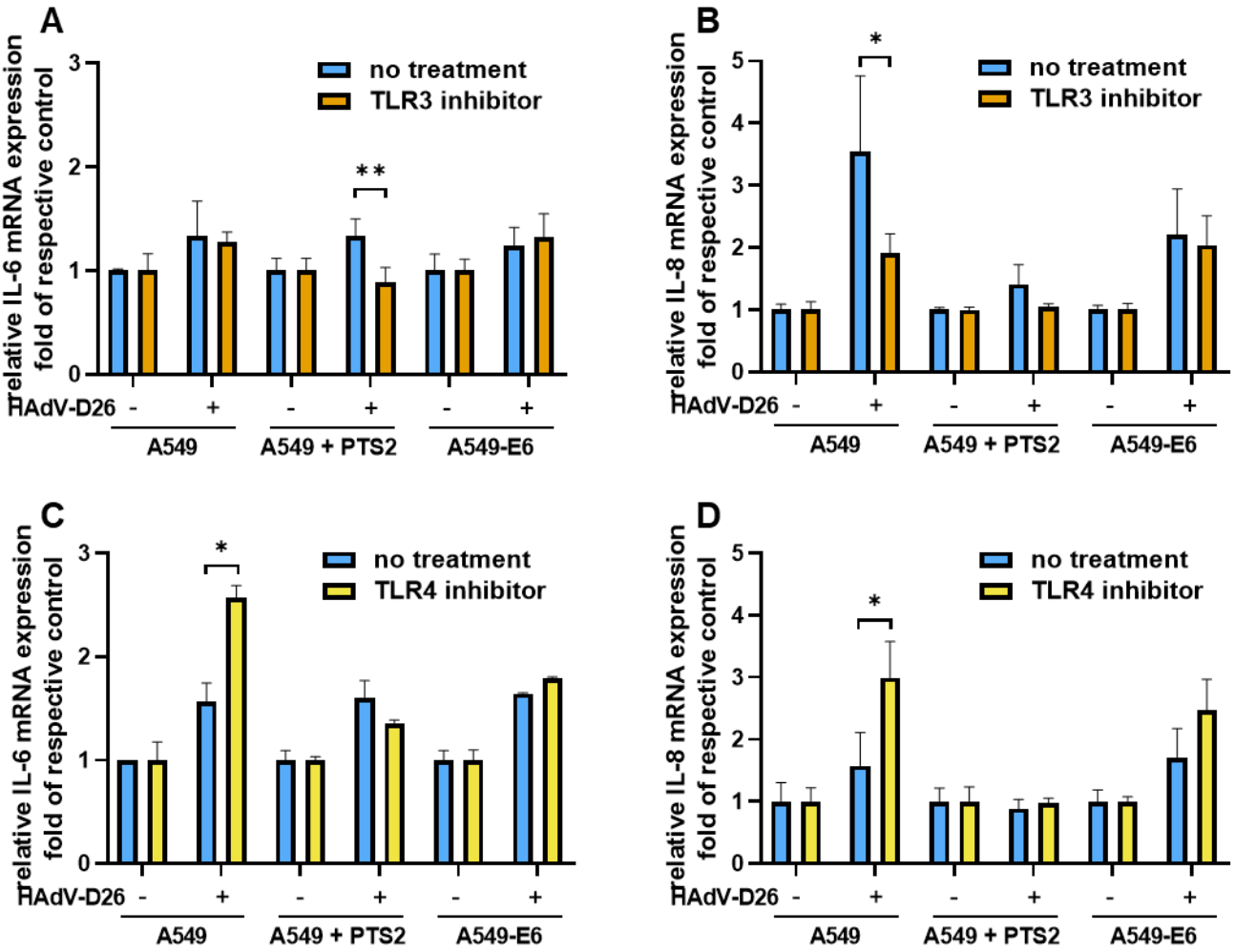


Figure 4. HAdV-D26-induced expression of IL-6 in CME-inhibited A549 cells and IL-8 in control A549 cells moderately depends on TLR3 activation. IL-6 and IL-8 mRNA levels measured by qPCR in TLR3- (A and B) or TLR4-inhibited (C and D) A549, CME-inhibited A549 (A549 + PTS2) or A549 cells with *de novo* expression of αvβ3 integrin (A549-E6) at 60 min p.i. with HAdV-D26 (MOI 10^4 vp/cell). Data are presented as mean ± SD, normalized to the control with no treatment and no virus.

p38 MAP kinase mediates HAdV-D26-induced IL-6 in CME-inhibited A549 cells. TLR signalling leads to activation of downstream MAP kinases [5]. In our previous research we saw that HAdV-D26 infection in human epithelial cells triggers the expression of pro-inflammatory cytokines and chemokines, including IL-6 and IL-8 [11]. We therefore examined the activation of MAPK pathways in CME-inhibited cells and cells with *de novo* expression of αvβ3 integrin following HAdV-D26 infection (Fig 5A and S3). While HAdV-D26 infection did not alter ERK phosphorylation in either CME-inhibited A549 cells or in cells with *de novo* expression of αvβ3 integrin, it increased p38 phosphorylation in both CME-inhibited A549 cells (1.4-fold) and A549 cells with *de novo* αvβ3 integrin expression (5.4-fold) (Fig. 5B).

Because we observed differential activation of the p38 signaling pathway in HAdV-D26–infected CME-inhibited A549 cells and A549 cells with *de novo* αvβ3 integrin expression, we next tested whether pharmacological inhibition of p38 would affect cytokine production. For that reason we pre-treated cells with the p38 inhibitor (SB203580) before infecting them with HAdV-D26. Inhibition of p38 (Fig. S2E) reduced IL-6 expression 2.7-fold in HAdV-D26 infected CME-inhibited A549 cells (Fig. 5C), but had no effect on IL-8 expression (Fig. 5D).

One of the p38 downstream targets in the context of regulating gene expression is NF-κB transcriptional factor [18], which can induce the synthesis of various pro-inflammatory cytokines [19]. Therefore, we determined NF-κB p65 nuclear translocation as indication of NF-κB pathway activation in HAdV-D26-infected CME-inhibited A549 cells or A549 cells with *de novo* αvβ3 integrin expression. 52% of CME-inhibited A549 cells showed NF-κB nuclear translocation 60 min p.i. with HAdV-D26, compared with 5% mock infected CME-inhibited A549 cells (Fig. S3). HAdV-D26 infection did not induce NF-κB p65 nuclear translocation, neither in A549 nor in A549 cells with *de novo* αvβ3 integrin expression. p38 MAPK signalling pathway has been reported to be involved also in regulating IFN gene expression following virus infection [20] however, in our cell model we did not observe IRF3 nuclear translocation (Fig. S3).

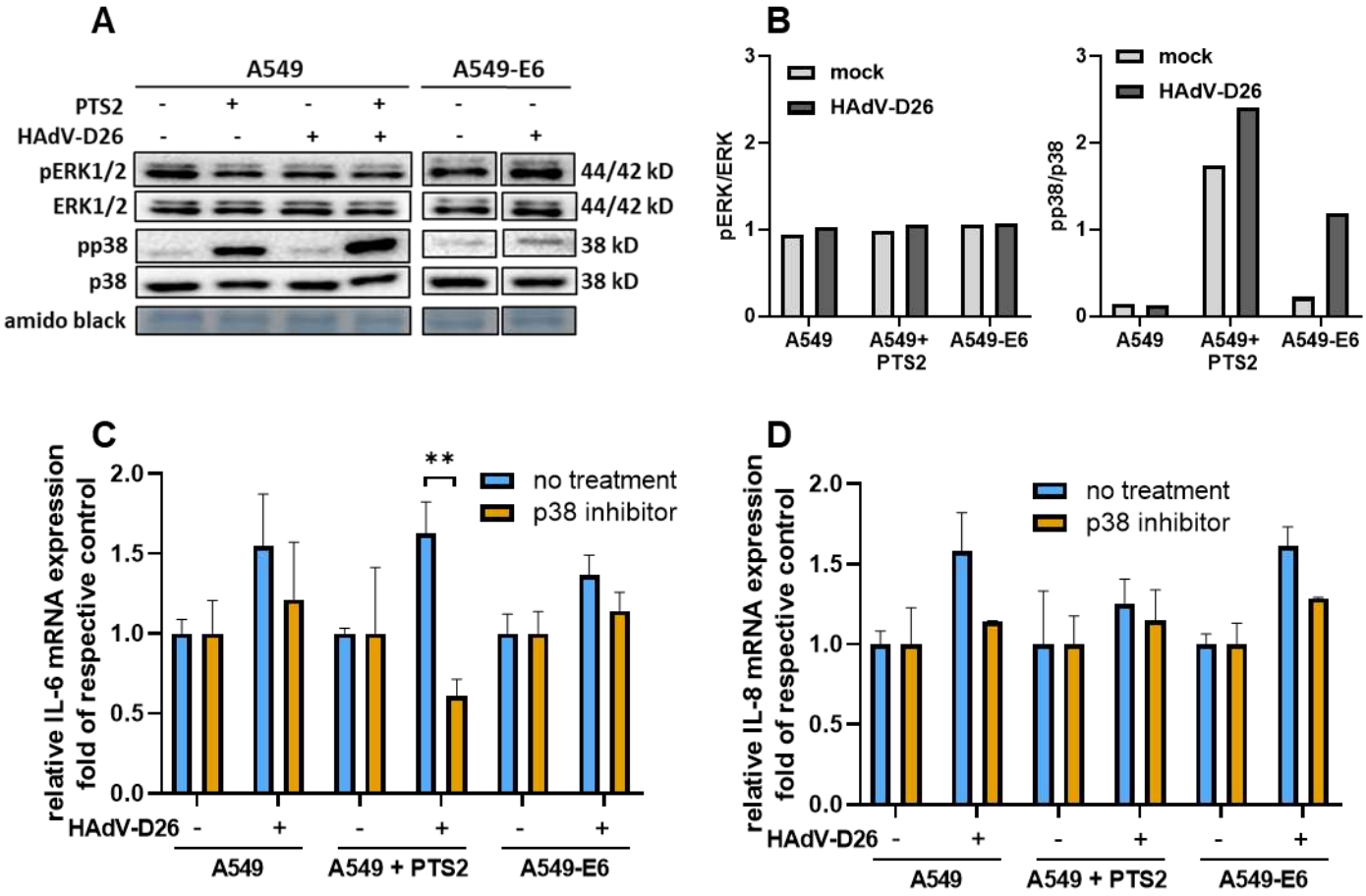


Figure 5. p38 MAP kinase partially mediates HAdV-D26–induced IL-6 expression in CME-inhibited A549 cells. (A) Representative Western blot and (B) corresponding

densitometric analysis of ERK1/2 and p38 phosphorylation in A549, CME-inhibited A549 (A549 + PTS2) or A549 cells with *de novo* expression of αvβ3 integrin (A549-E6) at 60 min p.i. with HAdV-D26 (MOI 10^4 vp/cell). One representative of two independent experiments is shown. Bands for A549-E6 were croped from different parts of the same membrane. (C) IL-6 and (D) IL-8 mRNA levels were measured by qPCR in p38-inhibited A549, CME-inhibited A549 (A549 + PTS2) or A549 cells with *de novo* expression of αvβ3 integrin (A549-E6) at 60 min p.i. with HAdV-D26 (MOI 10^4 vp/cell). Data are presented as mean ± SD, normalized to the control with no treatment and no virus.

Discussion.

In this study we investigated how the route of adenovirus entry and endosomal retention influences innate immune sensing and downstream inflammatory responses. Our results demonstrate that HAdV-D26-induced IL-6 and IL-8 expression is differentially regulated by distinct TLR pathways depending on whether CME is functional or not (Figure 6 and Table 2) highlighting viral entry as an important determinant of PRR engagement and cytokine induction during adenovirus infection.

Previously, we have shown that CME inhibition in A549 cell line stalled HAdV-D26 intracellular trafficking, indicating that in A549 cells with low expression of αvβ3 integrin, HAdV-D26 infection could be clathrin-mediated. In contrast, in A549 cells with *de novo* αvβ3 integrin expression, HAdV-D26 infection was shown to be caveolin-1-dependent [9]. The data presented here demonstrate that in CME-inhibited A549 cells, HAdV-D26 exhibits prolonged stay in early endosomes and lower localization in late endosomes/lysosomes than in A549 cells within the first hour of infection. Engaging αvβ3 integrin did not significantly change HAdV-D26 endosomal localization compared with A549 cells. In parallel, we saw increased IL-6 expression in HAdV-D26-infected CME-inhibited A549 cells, while *de novo* expression of αvβ3 integrin did not increase neither IL-6 nor IL-8 expression post HAdV-D26 infection, indicating that cytokine output is tightly linked to the subcellular context of viral sensing. Virus sensing mainly relies on detecting viral DNA and RNA through nucleic acid–sensing TLRs in endosomes and cytosolic sensors. TLR3 recognizes dsRNA, TLR7/8 detects ssRNA, and TLR9 senses CpG DNA, while some viral coat proteins activate surface TLRs (e.g., TLR2/6, TLR4) [21]. Prolonged retention within early endosomal compartments, as seen in CME-inhibited A549 cells, may increase the likelihood of HAdV-D26 exposure to endosomal PRRs, thereby influencing the magnitude and quality of downstream innate immune signaling. Excessive endosomal TLR signaling resulting from prolonged ligand–receptor contact has been described [22].

Adenovirus is a dsDNA virus, and TLR9, which senses foreign dsDNA, is the most commonly reported TLR to recognize adenoviruses. Because we were unable to achieve efficient TLR9 knockdown in our cell model, we instead investigated the role of its downstream adaptor protein, MyD88. MyD88 is the canonical adaptor for signaling pathways downstream of all TLRs except TLR3 [23]. MyD88 knockdown decreased only HAdV-D26-induced IL-8 expression in A549 cells with *de novo* expression of αvβ3 integrin, thereby linking αvβ3 integrin and caveolin-mediated HAdV-D26 entry [9] to MyD88-dependent signaling. It has been found that αvβ3 integrin boosts the recruitment of MyD88 to TLR2 [24], suggesting that HAdV-D26 usage of αvβ3 integrin could direct it toward TLRs other than TLR9. This is

consistent with the hypothesis that infectivity and cell entry alone are not sufficient for TLR9 recognition of adenoviruses; instead, such recognition depends on the use of a specific receptor-mediated entry pathway [15].

Next, we investigated the role of TICAM1, which functions downstream of TLR3 and also serves as an alternative adaptor in TLR4 signaling. TICAM1 knockdown reduced both HAdV-D26-induced IL-6 and IL-8 expression in CME-inhibited A549 cells, and IL-8 in A549 cells. These results are consistent with a model of cooperative innate sensing, indicating that TLR3 contributes to HAdV-D26-induced IL-6 and IL-8 expression but does not fully account for the enhanced cytokine response observed under CME inhibition. Involvement of TLR3 in inducing IL-6 expression in HAdV-D26-infected CME-inhibited cells was further corroborated by reduced IL-6 expression after inhibiting TLR3. TLR3 involvement has been reported in the HAdV-C5-mediated induction of MCP-1 and MIP-1β in mice [25]. TICAM1 knockdown did not affect HAdV-D26-induced IL-6 or IL-8 expression in A549 cells with *de novo* αvβ3 integrin expression. Similarly, TICAM1 or TLR3 signaling molecules were not required for HAdV-D26-based vaccine vector-induced cellular immunogenicity in mice [26]. Although TLR3 recognizes dsRNA, its activation in response to HAdV-D26 infection could be accounted by altered intracellular trafficking due to CME inhibition. Namely, CME inhibition may reroute HAdV-D26 to endosomal compartments enriched in TLR3, increasing the likelihood of TLR3 engagement. Prolonged stay of HAdV-D26 in early endosomes in CME-inhibited A549 cell HAdV-D26 might also allow extra time for virus degradation and subsequent sensing by TLR3. In addition, the crosstalk between viral RNA- and DNA-sensing mechanisms is also one possible explanation [27].

According to the literature TLR3 stimulation stands out as a promising strategy to (re)instance cancer immunosurveillance and demonstrated potential as an adjuvant to therapeutic tumor-targeting vaccines [28], but also as enhancer of antiviral immune responses [29]. In this context, our finding that HAdV-D26 induces TLR3 signaling in CME-inhibited cells suggests that this virus may possess intrinsic immunostimulatory properties that could serve as a blueprint for designing protein-based TLR3 agonists or vaccine vectors [30].

Finally, we identified p38 MAP kinase as a key signaling node mediating HAdV-D26-induced IL-6 expression in CME-inhibited A549 cells. One of the p38 downstream targets is NF-κB transcriptional factor [18] which can induce the synthesis of various pro-inflammatory cytokines [19]. We observed NF-κB nuclear translocation in more than 50% of HAdV-D26-infected CME-inhibited A549 supporting NF-κB activation. Contrary to our previous findings [11], under the conditions used in this study we did not observe activation of NF-κB in A549 cells following infection with HAdV-D26.

Unexpectedly, MyD88 knockdown or inhibiting TLR4 in A549 cells increased HAdV-D26 induced IL-6 and IL-8 expression implying that TLR4–MyD88 signalling has negative regulatory effect on pro-inflammatory cytokine production in these cells. The removal of this pathway may enhance signalling through MyD88-independent PPRs, such as cytosolic sensors, leading to amplified cytokine responses. The mechanism by which TLR4 functions as a negative regulator was described in HAdV-C5 infected murine liver [25]. A similar observation has been reported for TLR2 knockdown which increased IL-6 secretion in Cal-27 cells [31]. Interaction between TLR4 and adenoviruses was shown for HAdV-C5, -D26, and -B35 which in complex with lactoferrin [32] or neutrophil protein 1 [33] engage with TLR4 and induce

NLRP3 inflammasome formation. Further investigation of the TLR4 role in HAdV-D26-induced cytokine expression in A549 cells was beyond the scope of this study.

A key limitation of this study is the reliance on PTS2 for pharmacological CME inhibition, which can potentially impact clathrin-independent uptake pathways [34] thus, alternative approaches are needed in the future to more precisely isolate specific endocytic routes. Additionally, cytokine regulation was evaluated solely at the transcript level without direct analysis of protein secretion.

Collectively, our findings underscore the complexity of adenovirus innate immunity, which is often type- and cell-type dependent [35-38]. By demonstrating that HAdV-D26-induced IL-6 and IL-8 expression is differentially regulated by TLR3 or TLR4 signaling depending on the cell entry pathway, our data support a model in which adenovirus entry route and early trafficking events dictate PRR engagement, adaptor usage, and downstream signaling, thereby shaping the early innate immune response.

Table 2. Key findings reported in this study.

Cell model	Key alteration	Changes observed 60 min p.i. with HAdV-D26
A549	si(MyD88)	IL6 ↑ 4.2 fold IL8 ↑ 5.5 fold
	si(TICAM1)	IL8 ↓ 2.1 fold
	TLR3 inhibition	IL8 ↓ 1.9 fold
	TLR4 inhibition	IL6 ↑ 1.6 fold IL8 ↑ 1.9 fold
CME-inhibited A549 (A549+PTS2)	si(TICAM1)	IL6 ↓ 1.9 fold IL8 ↓ 1.5 fold
	TLR3 inhibition	IL6 ↓ 1.5 fold
	p38 inhibition	IL6 ↓ 2.7 fold
A549-E6 (*de novo* increased αvβ3 integrin)	si(MyD88)	IL8 ↓ 1.7 fold

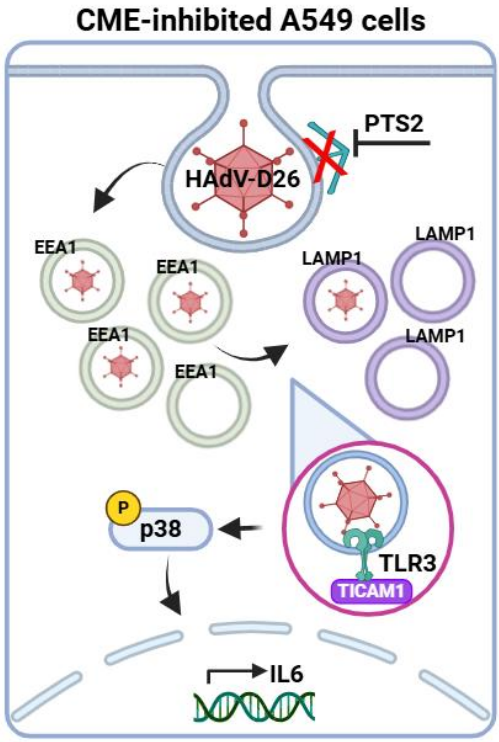


Figure 6. Proposed outline of TLR3-mediated IL-6 expression during early HAdV-D26 infection in epithelial cells under clathrin-mediated endocytosis inhibition. Inhibition of clathrin-mediated endocytosis redirects HAdV-D26 to prolonged retention in early endosomes (EEA1 positive, LAMP1 negative), which may facilitate activation of TLR3 signaling via TICAM-1, leading to p38 MAPK activation and subsequent induction of IL-6 expression. This illustration was created in BioRender (https://www.biorender.com/).

Materials and methods.

Cells and viruses. HEK293 (human embryonic kidney; ATCC CRL-1573) and A549 (human lung carcinoma; ATCC CCL-185) cells were obtained from ATCC and cultured according to the manufacturer's instructions. A549-E6 cells were previously generated in our laboratory [10]. A replication-incompetent recombinant HAdV-D26 vector carrying an enhanced green fluorescent protein was previously constructed [39] and fluorescently labelled as previously described [10].

Chemical inhibitors. Following inhibitors were used: CU-CPT 4a (final concentration 3 µM); TAK-242 (CLI-095, final concentration 0.5 µM); Adezmapimod (SB 203580, final concentration 100 µM); Pitstop 2 (PTS2, final concentration 20 µM). Stock solutions were prepared in DMSO. Working solutions were prepared in DMEM with 0.2% FBS. For all inhibitions pre-treatment of cells was done for 30 minutes at 37 °C.

Confocal and transmission electron microscopy. To assess HAdV-D26 localization to early and late endosomes/lysosomes, cells were seeded on glass coverslips (24-well plates; 2×10^4 cells/well) and two days later incubated with fluorescently labeled HAdV-D26 (MOI 10^4 vp/cell) on ice for 45 min to synchronize entry. Internalization was initiated by shifting to 37°C for 10 min, followed by removal of unbound virus and further incubation at 37°C for the indicated times. Cells were fixed, permeabilized, and stained with antibodies against EEA1

(#2411; Cell Signaling) or LAMP1 (ab24170; Abcam), followed by AF647 secondary antibody (#4414S; Cell Signaling) and AF555 phalloidin (#8953, Cell Signaling); nuclei were counterstained with DAPI. For imaging under CME inhibition, A549 cells were pre-treated with PTS2 and incubated with fluorescently labeled HAdV-D26 (MOI 10^4 vp/cell) for 60 min, with Weat Germ Agglutinin added during the final 5 min. Cells were washed, fixed, and mounted. Analysis was done by confocal microscopy (Leica TCS SP8 X, 63×/1.40 oil objective). Images were processed using LAS X software. For TEM analysis A549 cells grown on grids were infected with HAdV-D26 (MOI 2×10^5 vp/cell) on ice for 45 min and shifted to 37°C for 10 min. After washing, cells were incubated for 1 h at 37°C, fixed (2% glutaraldehyde/1% tannic acid in 0.4 M HEPES), dehydrated in ethanol, and processed for EPON embedding as described in [40]. Serial 70-nm sections from the basal 2 µm (4 sections/grid; 9 grids total) were stained with uranyl acetate and lead citrate and imaged using a JEOL JEM 1400 TEM (120 kV). Viral particles were quantified in 56 cells (>50 μm^2) in a unique section around 1 um of depth, and compartmental distribution was normalized to the total counted particles (n = 262).

Quantitative polymerase chain reaction (qPCR). Cells were seeded in 6-well plates (1×10^5 cells/well). After 48 h, cells were pre-treated with PTS2 and infected with HAdV-D26 (MOI 10^4 vp/cell) for 1 h at 37°C. Cells were harvested, and total RNA was extracted using the High Pure RNA Isolation Kit (Roche) and reverse-transcribed using the High-Capacity cDNA Reverse Transcription Kit (Applied Biosystems). qPCR was performed with SYBR Green on a StepOnePlus Real-Time PCR System. GAPDH served as a housekeeping gene. Primer sequences are: 1) *IL-6: Fw* CAATGAGGAGACTTGCCTGG, Rv GCACAGCTCTGGCTTGTTCC3; 2) *IL-8: Fw* GTTTTTGAAGAGGGCTGAGAATTC, *Rv* ATGAAGTGTTGAAGTAGATTTGCTTG3; 3) *GAPDH: Fw* AGAACATCATCCCTGCCTCTACTG, *Rv* TGTCGCTGTTGAAGTCAGAGGAGA; 4) *TICAM1: Fw* CAGGAGCCTGAGGAGATGAG, *Rv* CTGGGTAGTTGGTGCTGGTT; 5) MyD88: Fw TGCAGAGCAAGGAATGTGAC, Rv AGGATGCTGGGGAACTCTTT.

siRNA knockdown. A549 cells were transfected with siRNAs targeting MyD88 (10 nM; Ambion, 4390825) or TICAM1 (50 nM; Sigma-Aldrich, 12352203) using DharmaFECT 4 (Horizon Discovery) according to manufacturer instructions. Negative control siRNA (Silencer Select No. 1; Ambion, 4390844) was used as corresponding control. Cells were used 48 h post-transfection for qPCR or Western blot analyses.

SDS-PAGE and Western blot. Cells were seeded in 6-well plates (3×10^5 cells per well). After 48 h, cells were pre-treated with PTS2 and infected with HAdV-D26 (MOI 10^4 vp/cell) for 1 h. Cells were lysed and protein samples were separated on 10% SDS-PAGE gels and transferred onto nitrocellulose membranes. Membranes were incubated with specific primary antibodies (ERK, sc-94, Santa Cruz Biotechnology; pERK, sc-7383, Santa Cruz Biotechnology; p38, sc-535, Santa Cruz Biotechnology; pp38, sc-166182, Santa Cruz Biotechnology; MyD88 sc-74532, Santa Cruz Biotechnolog; NF-κB p65, L8F6, Cell Signaling; IRF-3, D6I4C, Cell Signaling) and appropriate HRP-conjugated secondary antibodies. Signal detection was performed using Pierce ECL Western Blotting Substrate (Thermo Fisher Scientific) and imaged with a ChemiDoc Imaging System (Bio-Rad). Densitometric analysis was conducted using ImageJ (v1.52a). Protein levels were normalized to amido black-stained membranes.

Statistical analysis. All experiments, except for TEM, were performed at least twice in duplicate or triplicate. Unless otherwise stated, average of at least two independent biological replicate with similar results is shown. All analyses and graphs were created in GraphPad Prism (GraphPad Software Inc., San Diego, CA, USA). Data were analyzed by unpaired Student's t-test, and expressed as mean ± standard deviation (SD). * $p < 0.05$; ** $p < 0.01$; *** $p < 0.001$; ns = non-significant ($p > 0.05$).

Literature

1. Scarsella, L., et al., *Advances of Recombinant Adenoviral Vectors in Preclinical and Clinical Applications.* Viruses, 2024. **16**(3): p. 377.
2. Nestić, D., et al. *The Revolving Door of Adenovirus Cell Entry: Not All Pathways Are Equal*. Pharmaceutics, 2021. **13**, DOI: 10.3390/pharmaceutics13101585.
3. Marquez-Martinez, S., et al., *Cell entry and innate sensing shape adaptive immune responses to adenovirus-based vaccines.* Current Opinion in Immunology, 2023. **80**: p. 102282.
4. Brubaker, S.W., et al., *Innate Immune Pattern Recognition: A Cell Biological Perspective.* Annual Review of Immunology, 2015. **33**(Volume 33, 2015): p. 257-290.
5. Kawai, T., et al., *Decoding Toll-like receptors: Recent insights and perspectives in innate immunity.* Immunity, 2024. **57**(4): p. 649-673.
6. Bonhomme, D. and E.Z. Poirier, *Early signaling pathways in virus-infected cells.* Current Opinion in Virology, 2024. **66**: p. 101411.
7. Chen, R., et al., *Pattern recognition receptors: function, regulation and therapeutic potential.* Signal Transduction and Targeted Therapy, 2025. **10**(1): p. 216.
8. Majhen, D., *Human adenovirus type 26 basic biology and its usage as vaccine vector.* Reviews in Medical Virology, 2022. **32**(6): p. e2338.
9. Nestić, D., et al., *Human Adenovirus Type 26 Infection Mediated by αvβ3 Integrin Is Caveolin-1-Dependent.* Microbiology Spectrum, 2022. **10**(4): p. e01097-22.
10. Nestić, D., et al., *αvβ3 Integrin Is Required for Efficient Infection of Epithelial Cells with Human Adenovirus Type 26.* J Virol, 2019. **93**(1).
11. Nestić, D., et al., *Human Adenovirus Type 26 Induced IL-6 Gene Expression in an αvβ3 Integrin- and NF-κB-Dependent Manner.* Viruses, 2022. **14**(4): p. 672.
12. Sartorius, R., et al., *Exploiting viral sensing mediated by Toll-like receptors to design innovative vaccines.* npj Vaccines, 2021. **6**(1): p. 127.
13. Shirley, J.L., et al., *Immune Responses to Viral Gene Therapy Vectors.* Molecular Therapy, 2020. **28**(3): p. 709-722.
14. von Kleist, L., et al., *Role of the Clathrin Terminal Domain in Regulating Coated Pit Dynamics Revealed by Small Molecule Inhibition.* Cell, 2011. **146**(3): p. 471-484.
15. Iacobelli-Martinez, M. and G.R. Nemerow, *Preferential Activation of Toll-Like Receptor Nine by CD46-Utilizing Adenoviruses.* Journal of Virology, 2007. **81**(3): p. 1305-1312.
16. Cerullo, V., et al., *Toll-like Receptor 9 Triggers an Innate Immune Response to Helper-dependent Adenoviral Vectors.* Molecular Therapy, 2007. **15**(2): p. 378-385.
17. Piras, V. and K. Selvarajoo, *Beyond MyD88 and TRIF Pathways in Toll-Like Receptor Signaling.* Frontiers in Immunology, 2014. **Volume 5 - 2014**.
18. Carter, A.B., et al., *The p38 Mitogen-activated Protein Kinase Is Required for NF-κB-dependent Gene Expression: THE ROLE OF TATA-BINDING PROTEIN (TBP) **.* Journal of Biological Chemistry, 1999. **274**(43): p. 30858-30863.
19. Guo, Q., et al., *NF-κB in biology and targeted therapy: new insights and translational implications.* Signal Transduction and Targeted Therapy, 2024. **9**(1): p. 53.

20. Jiang, M., et al., *MAP kinase p38α regulates type III interferon (IFN-λ1) gene expression in human monocyte-derived dendritic cells in response to RNA stimulation.* J Leukoc Biol, 2015. **97**(2): p. 307-20.
21. Carty, M., C. Guy, and A.G. Bowie, *Detection of Viral Infections by Innate Immunity.* Biochemical Pharmacology, 2021. **183**: p. 114316.
22. McAlpine, W., et al., *Excessive endosomal TLR signaling causes inflammatory disease in mice with defective SMCR8-WDR41-C9ORF72 complex function.* Proceedings of the National Academy of Sciences, 2018. **115**(49): p. E11523-E11531.
23. Deguine, J. and G.M. Barton, *MyD88: a central player in innate immune signaling.* F1000Prime Rep, 2014. **6**: p. 97.
24. Gianni, T. and G. Campadelli-Fiume, *The Epithelial αvβ3-Integrin Boosts the MYD88-Dependent TLR2 Signaling in Response to Viral and Bacterial Components.* PLOS Pathogens, 2014. **10**(11): p. e1004477.
25. Appledorn, D.M., et al., *TRIF, and TRIF-interacting TLRs differentially modulate several adenovirus vector-induced immune responses.* J Innate Immun, 2009. **1**(4): p. 376-88.
26. Rhee, E.G., et al., *Multiple Innate Immune Pathways Contribute to the Immunogenicity of Recombinant Adenovirus Vaccine Vectors.* Journal of Virology, 2011. **85**(1): p. 315-323.
27. Cai, C., et al., *The crosstalk between viral RNA- and DNA-sensing mechanisms.* Cellular and Molecular Life Sciences, 2021. **78**(23): p. 7427-7434.
28. Le Naour, J., et al., *Trial watch: TLR3 agonists in cancer therapy.* OncoImmunology, 2020. **9**(1): p. 1771143.
29. Shao, F., et al., *TLR agonists as adjuvants for viral vaccines: mechanisms, applications, and future directions.* Frontiers in Microbiology, 2026. **Volume 16 - 2025**.
30. Adams, C.S., et al., *De novo design of protein minibinder agonists of TLR3.* Nature Communications, 2025. **16**(1): p. 1234.
31. Koch, A.T., et al., *MyD88-Dependent Signaling Decreases the Antitumor Efficacy of Epidermal Growth Factor Receptor Inhibition in Head and Neck Cancer Cells.* Cancer research, 2015. **75**(8): p. 1657-1667.
32. Chéneau, C., et al., *Lactoferrin Retargets Human Adenoviruses to TLR4 to Induce an Abortive NLRP3-Associated Pyroptotic Response in Human Phagocytes.* Frontiers in Immunology, 2021. **Volume 12 - 2021**.
33. Eichholz, K., et al., *Adenovirus-α-Defensin Complexes Induce NLRP3-Associated Maturation of Human Phagocytes via Toll-Like Receptor 4 Engagement.* Journal of Virology, 2022. **96**(6): p. e01850-21.
34. Dutta, D., et al., *Pitstop 2 Is a Potent Inhibitor of Clathrin-Independent Endocytosis.* PLOS ONE, 2012. **7**(9): p. e45799.
35. Hartman, Z.C., E.P. Black, and A. Amalfitano, *Adenoviral infection induces a multi-faceted innate cellular immune response that is mediated by the toll-like receptor pathway in A549 cells.* Virology, 2007. **358**(2): p. 357-372.
36. Appledorn, D.M., et al., *Adenovirus Vector-Induced Innate Inflammatory Mediators, MAPK Signaling, As Well As Adaptive Immune Responses Are Dependent upon Both TLR2 and TLR9 In Vivo1.* The Journal of Immunology, 2008. **181**(3): p. 2134-2144.
37. Nociari, M., et al., *Sensing Infection by Adenovirus: Toll-Like Receptor-Independent Viral DNA Recognition Signals Activation of the Interferon Regulatory Factor 3 Master Regulator.* Journal of Virology, 2007. **81**(8): p. 4145-4157.
38. Zhu, J., X. Huang, and Y. Yang, *Innate Immune Response to Adenoviral Vectors Is Mediated by both Toll-Like Receptor-Dependent and -Independent Pathways.* Journal of Virology, 2007. **81**(7): p. 3170-3180.
39. Abbink, P., et al., *Comparative seroprevalence and immunogenicity of six rare serotype recombinant adenovirus vaccine vectors from subgroups B and D.* J Virol, 2007. **81**(9): p. 4654-63.

40. Menéndez-Conejero, R., et al., *Biophysical methods to monitor structural aspects of the adenovirus infectious cycle.* Methods Mol Biol, 2014. **1089**: p. 1-24.

Acknowledgment

D.M. acknowledges funding from Croatia Science Foundation Research Projects (Grant IP-2019-04-6048 and IP-2025-02-3470 to D.M.); C.S.M. acknowledges funding from the Spanish State Research Agency, with co-funding from the European Regional Development Fund (PID2022-136456NB-I00/AEI/10.13039/501100011033). The C.S.M. group is a member of the Spanish Adenovirus Network (RED2022-134221-T/AEI/10.13039/501100011033). CNB-CSIC is an AEI Severo Ochoa Excellence Center (CEX2023-001386-S/AEI/10.13039/501100011033). Support from the European Commission Marie Skłodowska-Curie Actions (grant agreement 101129778, project INVECTA) to D.M. and C.S.M. is also acknowledged.

We thank the CNB-CSIC Electron Microscopy and Advanced Optical Microscopy facilities for the excellent technical support.

Author contributions

Conceptualization: Isabela Drašković, Lea Vrbančić, Davor Nestić, Dragomira Majhen
Data curation: Dragomira Majhen
Formal analysis: Isabela Drašković, Lea Vrbančić, Davor Nestić, Ksenija Božinović, Gabriela N. Condezo, Dragomira Majhen
Funding acquisition: Dragomira Majhen
Investigation: Isabela Drašković, Lea Vrbančić, Davor Nestić, Gabriela N. Condezo
Methodology: Isabela Drašković, Lea Vrbančić, Davor Nestić, Ksenija Božinović, Gabriela N. Condezo, Carmen San Martín, Jerome Custers, Dragomira Majhen
Resources: Carmen San Martín, Jerome Custers, Dragomira Majhen
Supervision: Dragomira Majhen
Visualization: Isabela Drašković, Lea Vrbančić. Davor Nestić, Gabriela N. Condezo
Writing – original draft: Isabela Drašković, Dragomira Majhen
Writing – review & editing: Isabela Drašković, Lea Vrbančić, Davor Nestić, Ksenija Božinović, Gabriela N. Condezo, Carmen San Martín, Dragomira Majhen

Data Availability

All data generated or analysed during this study are included in this published article [and its supplementary information files].

Supplementary figures

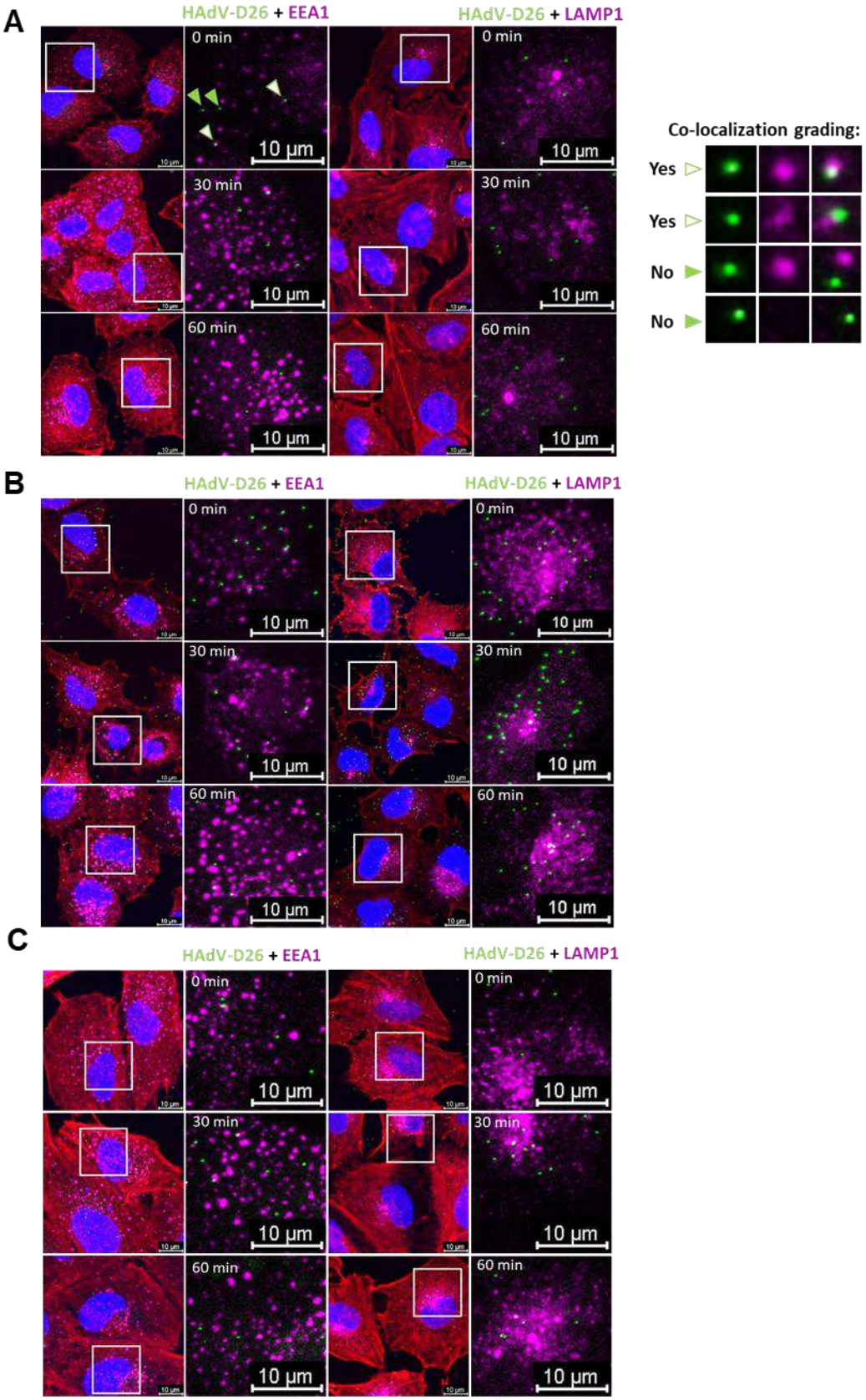


Figure S1. Localization of HAdV-D26 within early or late endosome/lysosome during 60 minutes of internalization. Representative confocal images of HAdV-D26 localization in EEA1-positive (early) or LAMP1-positive (late) endosome in (A) A549, (B) CME-inhibited A549 (A549 + PTS2) and (C) A549 cells with *de novo* expression of αvβ3 integrin (A549-E6) during 60 min of internalization. Green, virus; red, cell membrane; blue, nucleus; purple, EEA1/LAMP1.

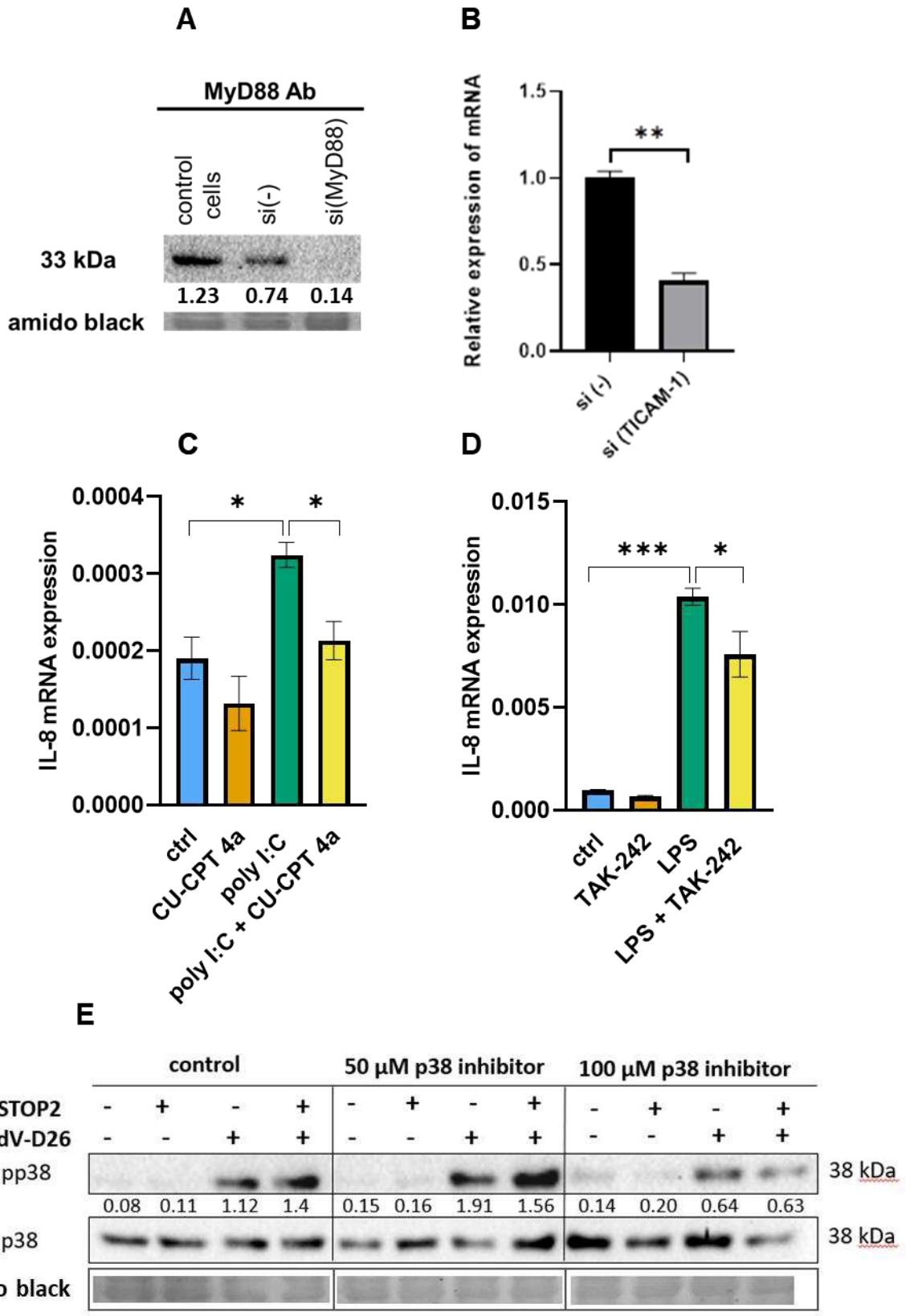
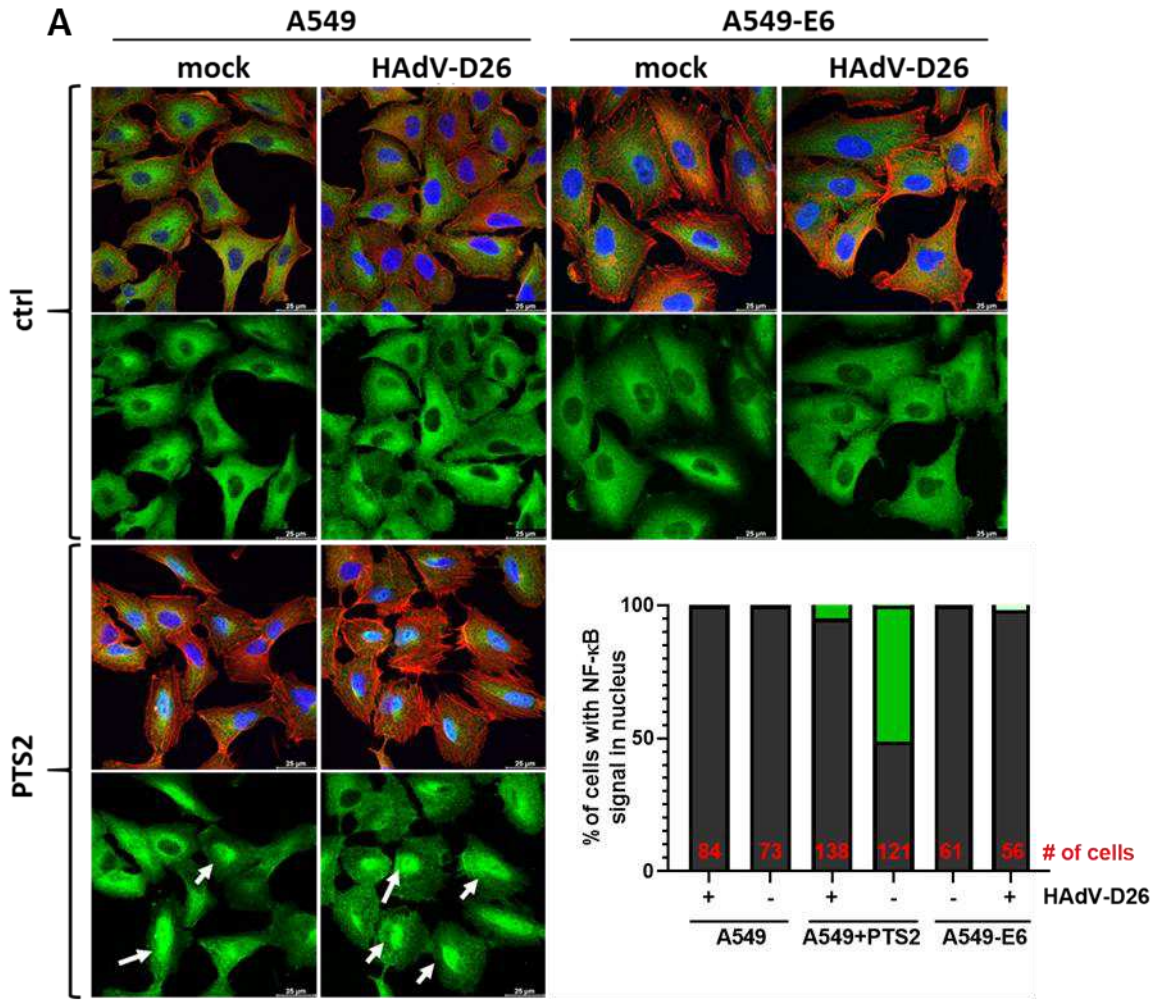
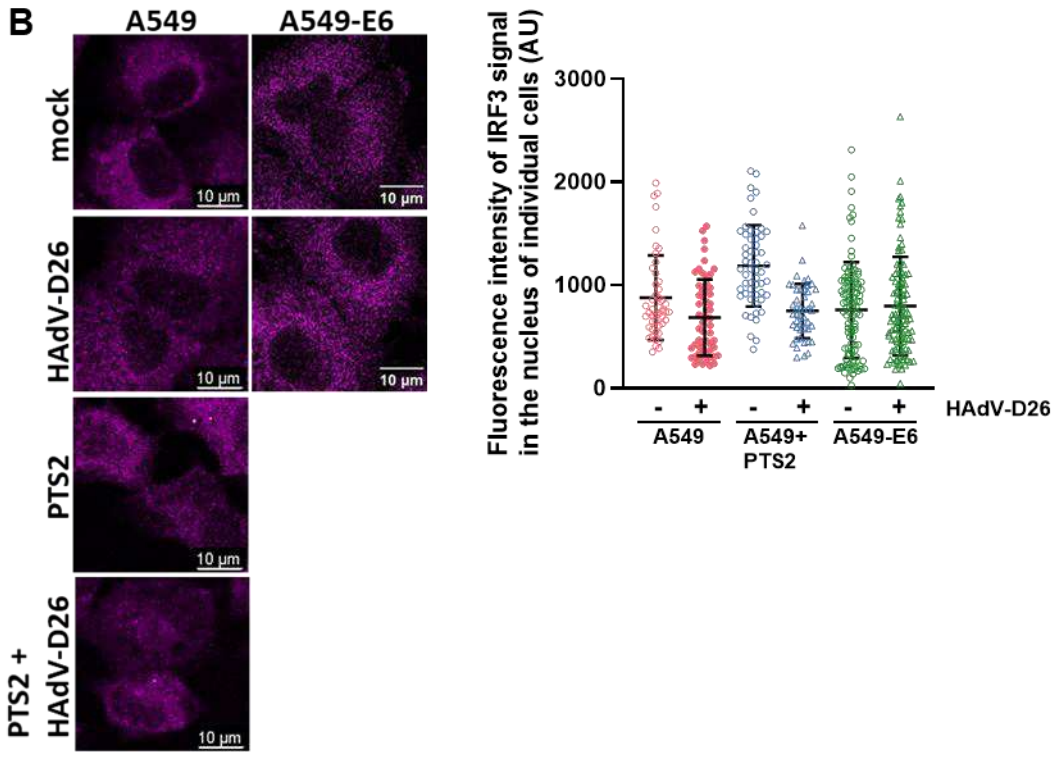


Figure S2. The efficacy of MyD88 and TICAM-1 downregulation, and p38, TLR3, and TLR4 inhibition. (A) Expression of MyD88 in A549 cells after downregulating with specific

siRNA. The numbers below the bands are obtained by densitometric analysis of chemiluminescent signals of MyD88 relative to amido black staining. A representative result from one of three independent experiments with similar outcomes is shown. (B) The efficacy of TICAM1 knockdown in A549 cells was assessed by qPCR using gene-specific primers. Forty-eight hours after transfection with siTICAM1, total RNA was extracted from the cells and reverse-transcribed into cDNA. TICAM1 mRNA levels were then quantified by qPCR. Data were normalized to the endogenous control GAPDH and to control cells transfected with non-targeting siRNA. (C) Efficacy of TLR3 inhibition in A549 cells. IL-8 expression in A549 cells following poly I:C stimulation with or without TLR3 inhibitor (CU-CPT 4a) was analysed by qPCR. Results were normalized to the endogenous control GAPDH and shown as fold of control cells treated with inhibitor. (D) Efficacy of TLR4 inhibition in A549 cells. IL-8 expression in A549 cells following LPS stimulation with or without TLR4 inhibitor (TAK-242) was analyzed by qPCR. Results were normalized to the endogenous control GAPDH and shown as fold of control cells treated with inhibitor. (E) The efficacy of p38 inhibition in A549 cells. Activation of p38 kinase in A549 cells following PTS2 treatment and/or HAdV-D26 transduction with or without p38 inhibitor (Adezmapimod – SB203580) analyzed by SDS-PAGE and Western blotting. The results obtained by densitometric analysis of chemiluminescent signals of p38 MAP kinase are presented as numerical values indicating the ratio of phosphorylated to total (non-phosphorylated) protein. Amido black staining of the membrane shows equal loading of protein samples. A representative result from one of three independent experiments with similar outcomes is shown.


A
A549
A549-E6
mock
HAdV-D26
mock
HAdV-D26
ctrl
PTS2
% of cells with NF-κB signal in nucleus
100
50
0
84
73
138
121
61
56
# of cells
+
-
+
-
-
+
HAdV-D26
A549
A549+PTS2
A549-E6


B
A549
A549-E6
mock
HAdV-D26
PTS2
PTS2 + HAdV-D26
10 µm
Fluorescence intensity of IRF3 signal in the nucleus of individual cells (AU)
3000
2000
1000
0
- + - + - +
HAdV-D26
A549
A549+ PTS2
A549-E6

569

Figure S3. HAdV-D26 infection of CME-inhibited A549 cells activates NF-κB. (A) Representative confocal images and corresponding quantification analysis of NF-κB translocation in cell nucleus of A549, CME-inhibited A549 (A549 + PTS2) or A549 cells with *de novo* expression of αvβ3 integrin (A549-E6) at 60 min p.i. with HAdV-D26 (MOI 10^4 vp/cell). White arrows indicate signal in nucleus. (B) Representative confocal images and corresponding quantification analysis of IRF3 translocation presented as mean fluorescence intensity of individual cell nuclei of A549, CME-inhibited A549 (A549 + PTS2) or A549 cells with *de novo* expression of αvβ3 integrin (A549-E6) at 60 min p.i. with HAdV-D26 (MOI 10^4 vp/cell).

Supplementary Files

This is a list of supplementary files associated with this preprint. Click to download.

- DrakovietalSciReportswesternblotsoriginal.pdf